A 1500-year El Niño/Southern Oscillation and rainfall history for the Isthmus of Panama from speleothem calcite

Matthew S. Lachniet,[1] Stephen J. Burns,[2] Dolores R. Piperno,[3] Yemane Asmerom,[4] Victor J. Polyak,[4] Christopher M. Moy,[5] and Keith Christenson[6]

Received 25 February 2004; revised 28 May 2004; accepted 6 August 2004; published 30 October 2004.

[1] The effect of the El Niño/Southern Oscillation (ENSO) on tropical rainfall variations of the past 2 millennia is largely unknown. High-resolution monsoon records are sparse, despite the role of ENSO in generating global hydrologic anomalies in modern climate. To investigate the relationship between ENSO and the Central American Monsoon, we generated a high-resolution (~2.9 years/sample) oxygen-isotope monsoon rainfall record from a U/Th-dated stalagmite (180 B.C. to 1310 A.D.) from the Isthmus of Panama. We present evidence for a weakened monsoon during the "High Medieval" (1100–1200 A.D.) and the Classic Maya Collapse (750–950 A.D.). Rainfall decreased and was more variable after 550 A.D., and the period 900–1310 A.D. was drier than the preceding millennium. A weaker monsoon corresponds with increased El Niño variability, and our data display statistical variance in the ENSO band. We conclude that ENSO variation has forced isthmian rainfall and may have contributed to hemispheric climatic anomalies at this time. *INDEX TERMS:* 1040 Geochemistry: Isotopic composition/chemistry; 1620 Global Change: Climate dynamics (3309); 1854 Hydrology: Precipitation (3354); 3344 Meteorology and Atmospheric Dynamics: Paleoclimatology; 3339 Meteorology and Atmospheric Dynamics: Ocean/atmosphere interactions (0312, 4504); *KEYWORDS:* paleoclimate, El Niño/Southern Oscillation, speleothem, Medieval Climatic Anomaly, Intertropical Convergence Zone, Panama

Citation: Lachniet, M. S., S. J. Burns, D. R. Piperno, Y. Asmerom, V. J. Polyak, C. M. Moy, and K. Christenson (2004), A 1500-year El Niño/Southern Oscillation and rainfall history for the Isthmus of Panama from speleothem calcite, *J. Geophys. Res.*, *109*, D20117, doi:10.1029/2004JD004694.

1. Introduction

[2] Dry anomalies linked to the demise of the Maya have been linked to solar variability [*Hodell et al.*, 2001], based on sediment cores from the Yucatan, and to variations in the mean position of the Intertropical Convergence Zone (ITCZ) as inferred from variations in riverine Ti concentrations in a sediment core from the Cariaco Basin [*Haug et al.*, 2003]. Further, evidence for tropical hydrologic anomalies is sparse during medieval time [*Bradley et al.*, 2003], despite evidence for climatic anomalies at midlatitudes such as warm European temperatures [*Lamb*, 1965] and pronounced drought in California and Patagonia [*Stine*, 1994]. However, the potential role of the eastern equatorial Pacific Ocean and ENSO in producing hydrologic anomalies in Panama during the past 2 millennia has not been investigated. On timescales beyond the period of instrumental records, the relationship between monsoonal rainfall, rainfall $\delta^{18}O$ values, and variation in ENSO is poorly known, particularly in Central America. To test the possible role of ENSO in generating regional hydrologic anomalies in Central America, we generated a high-resolution (~2.9 years/sample), speleothem-based $\delta^{18}O$ monsoon rainfall history from the Isthmus of Panama (Figure 1), a region that responds strongly to ENSO events via monsoon intensity variations. Stalagmite CHIL-1 is a 49-cm-tall conical stalagmite collected beneath an active slow drip ~75 m within Chilibrillo Cave in eastern Panama (9.2°N, 79.7°W), located ~30 km from the Pacific Coast at an elevation of 60 m.

[3] Speleothem-based ENSO paleoclimate records can complement those derived from corals. For example, speleothems may record terrestrial paleoclimate at an annual resolution near that of corals [*Polyak and Asmerom*, 2001], and may grow continuously for several thousand years. Although corals may be sampled at subannual resolution, they typically grow over short time intervals, and the most complete records are obtained by splicing together several "floating" coral time series [e.g., *Cobb et al.*, 2003] that commonly contain significant time gaps in coverage. Also, during some very strong warm El Niño events, coral bleaching may preclude preservation of an isotopic signal

[1]Department of Geoscience, University of Nevada, Las Vegas, Nevada, USA.
[2]Department of Geosciences, University of Massachusetts, Amherst, Massachusetts, USA.
[3]Smithsonian Tropical Research Institute, Balboa, Republic of Panama.
[4]Department of Earth and Planetary Sciences, University of New Mexico, Albuquerque, New Mexico, USA.
[5]Department of Geological and Environmental Sciences, Stanford University, Stanford, California, USA.
[6]Falls Church, Virginia, USA.

0148-0227/04/2004JD004694$09.00

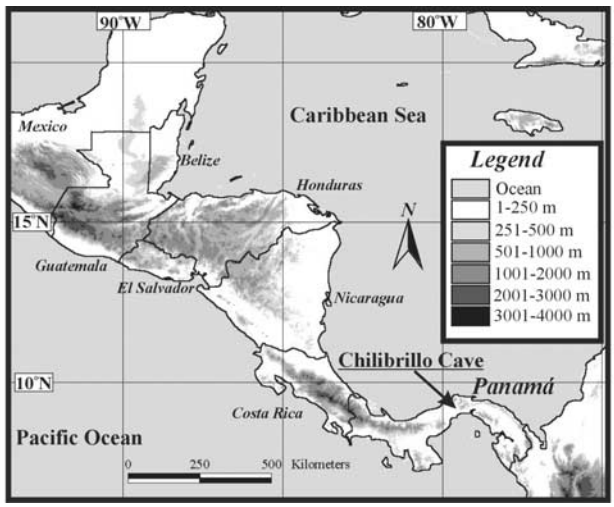

Figure 1. Site map digital elevation model of Central America and location of Chilibrillo Cave, Canal Zone, Panama.

[*Linsley et al.*, 1994], and local oceanographic conditions result in competing dominance of sea surface salinity and sea surface temperature on the coral $\delta^{18}O$ values. The $\delta^{18}O$ records from tropical stalagmites can provide monsoon rainfall histories that will be useful in evaluating paleoclimate of the past 2 millennia. Speleothems are useful paleoclimate proxies because they incorporate rainfall-derived oxygen into precipitated $CaCO_3$, and can be precisely dated by U-series isotopes [*Hendy*, 1971; *Richards and Dorale*, 2003]. In tropical regions where rainfall is dominated by strong vertical convection, rainfall $\delta^{18}O$ values are inversely correlated with rainfall amount via the amount effect [*Rozanski et al.*, 1993]. Thus, speleothem calcite $\delta^{18}O$ should preserve a high-resolution signal of past rainfall $\delta^{18}O$ variations [*Burns et al.*, 2002; *Fleitmann et al.*, 2003], and we interpret the $\delta^{18}O$ stratigraphy of stalagmite sample CHIL-1 from Chilibrillo Cave, Panama, as a rainfall proxy.

[4] Kinetic effects may also perturb the $\delta^{18}O$ and $\delta^{13}C$ values of stalagmite carbonate. In caves with high relative humidity, the most likely source of kinetic fractionation would be due to rapid degassing of CO_2. Such a kinetic effect works in the same "direction" as the amount effect [*Burns et al.*, 2002], in that drier climate will result in less drip water delivery to the stalagmite, a thinner water film, enhanced CO_2 degassing, and increased $\delta^{18}O$ and $\delta^{13}C$ values [*Hendy*, 1971]. Variations in soil respiration rate and CO_2 recycling linked to historical El Niño events have also been inferred from $\delta^{13}C$ values in a stalagmite from Belize [*Frappier et al.*, 2002].

[5] The climate of southern Central America is dominated by the annual migration of the ITCZ and the Central American Monsoon (CAM) [*Giannini et al.*, 2000]. The climate cycle at the cave site is defined by alternating wet (April to November) and dry (December to March) seasons. Mean annual precipitation is 2400 mm, and mean annual temperature is 27.0°C [*Windsor*, 1990]. The ENSO is the largest source of interannual climate variability in the tropics [*Hastenrath*, 1978, 1984; *Ropelewski and Halpert*, 1987; *Waylen et al.*, 1996].

[6] In Panama, the climatic response to El Niño events over the period of instrumental record is a weakening of the monsoon and decreased rainfall in the ITCZ, an increase in the length of the following dry season, and a water deficit in the Panama Canal system (M. Donoso et al., Panama Canal case study: Impacts and responses to the 1997–98 El Niño event, available at http://www.esig.ucar.edu/un/panama_canal.html, 2003, accessed 26 May 2004, hereinafter referred to as Donoso et al., Panama Canal case study, 2003). The dry season in Panama is longer during El Niño events, especially if the tropical North Atlantic is cool [*Enfield and Alfaro*, 1999]. *Estoque et al.* [1985] demonstrated that 11 of 12 El Niño events were associated with below-average rainfall and decreased river runoff to the Panama Canal. For example, the water level of artificial Lago Gatun (Figure 2) records a basin-wide integrated signal of rainfall in the Panama Canal Zone and Chilibrillo Cave area from 1971 to 2001, which spans the pronounced El Niño events of 1972/1973, 1976, 1982/1983 and 1997/1998 (data available at http://striweb.si.edu/esp/). Rainfall anomalies in climate stations in the Canal area were −30% in 1976, −24% in 1982, and −35% in 1998 [*Estoque et al.*, 1985; Donoso et al., Panama Canal case study, 2003]. Anomalously short rainy seasons (exceeding 2σ of mean) in 1976, 1982, and 1997 preceded low lake levels, and the following dry seasons were anomalously long. Comparison of Gatun lake levels and the NINO3 (5°N–5°S, 150°–90°W) sea surface temperature (SST) data (available at http://www.cpc.ncep.noaa.gov/data/indices/) in Figure 2 reveals that pronounced warming in the eastern equatorial Pacific Ocean is associated with reduced lake levels in the Panama Canal Zone. Anomalously low lake levels are prominent in 1973, 1976/1977, 1983, and 1997/1998, all of which are associated with El Niño events. Although freshwater from Lago Gatun is diverted to fill the Panama Canal lock system, lake level fluctuations have a dominantly climatic origin (Donoso, Panama Canal case study, 2003). The modern ENSO/climate relationship is supported by and extended to 1707 A.D. with a coral $\delta^{18}O$ time series

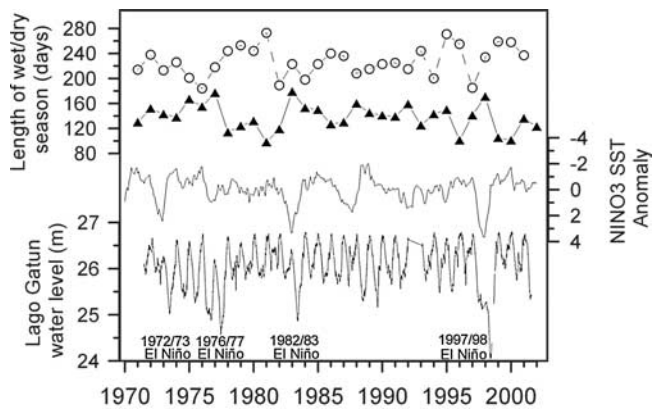

Figure 2. Comparison of Gatun Lake levels with NINO3 (5°N–5°S, 150°–90°W) sea surface temperature (SST) anomalies and the length of the wet (circles) and dry (triangles) seasons in Panama. Anomalously warm eastern equatorial Pacific SSTs are associated with decreased wet season rainfall, a longer dry season, and lowered Gatun Lake levels.

Table 1. U-Series Isotopic Ratios and $^{230}Th/^{234}U$ Ages for Sample CHIL-1

Sample Identification	Distance From Base, mm	^{238}U, ppm	±2σ	^{232}Th, ppb	±2σ	$^{230}Th/^{232}Th$ (Atomic)	±2σ	$\delta^{234}U$ Measured,[a] ‰	±2σ	$^{230}Th/^{238}U$ (Activity)	±2σ	Age, years BP	±2σ	Age, years A.D./B.C.
102	18	0.5458	0.0041	1.276	0.020	114.7	2.02	−159.4	9.3	0.01636	0.00047	2066	77	64 B.C.
96	117	0.5646	0.0031	1.750	0.017	80.6	0.90	−117.4	3.9	0.01525	0.00063	1801	96	201 A.D.
97	210	0.5404	0.0041	0.531	0.016	174.1	5.55	−125.2	5.5	0.01040	0.00148	1274	188	728 A.D.
123	398	0.4598	0.0025	0.509	0.016	108.6	3.56	−116.9	5.3	0.00729	0.00086	868	106	1134 A.D.
111	477	0.4482	0.0028	0.309	0.019	134.2	8.22	−122.7	5.8	0.00564	0.00079	681	99	1321 A.D.

[a]The $\delta^{234}U_{measured} = [(^{234}U/^{238}U)_{measured}/(^{234}U/^{238}U)_{eq} - 1] \times 10^3$, where $(^{234}U/^{238}U)_{eq}$ is the secular equilibrium atomic ratio, which is $\lambda_{238}/\lambda_{234} = 5.48862 \times 10^{-5}$.

from the Gulf of Chiriquí, Panama [*Linsley et al.*, 1994]. These data demonstrate interannual $\delta^{18}O$ variability with dominant variance at 9 and 3–7 years (ENSO band), and the authors also note that ENSO band variance is present in Panamanian rainfall data.

2. Methods

[7] The stalagmite was halved, polished, and five ~300-mg subsamples were analyzed for U-series isotopes at the University of New Mexico Radiogenic Isotope Laboratory (Table 1). Stalagmite powder was dissolved in HNO_3 and spiked with a mixed ^{229}Th-^{233}U-^{236}U spike. The use of a mixed spike eliminates propagation of weighting error into the age uncertainties. U and Th were coprecipitated with $FeOH_3$ and separated in anion exchange columns in two steps. Isotopic ratios were measured on a Micromass Sector 54 thermal ionization mass spectrometer with a high-abundance sensitivity filter using an ion-counting Daly multiplier. The reported uncertainties in the ratios are 2σ of the mean. Age uncertainties include uncertainties related to initial $^{230}Th/^{232}Th$ correction, which is $4.4 \times 10^{-6} \pm 50\%$ assuming a silicate component with bulk silicate earth (BSE) $^{232}Th/^{238}U$ ratio of 3.8. The calculated ages and growth rates vary slightly depending on the choice of the initial $^{230}Th/^{232}Th$ ratio, e.g., 0.373 mm/yr for the BSE-based $^{230}Th/^{232}Th$ initial, and 0.339 mm/yr for a $^{230}Th/^{232}Th$ initial of 1.0×10^{-5}. Measurements of layer thickness, suspected to be annual, in thin sections made from the bottom 150 mm of CHIL-1 and bracketed by two U/Th dates, yielded an average layer thickness of 0.378 mm. This value corresponds well with the average growth rate of 0.373 mm/yr, determined by linear interpolation between the U/Th ages (samples 102 and 96) calculated with a $^{230}Th/^{232}Th$ ratio of 4.4×10^{-6}. The concordance of growth rates estimated from U/Th dating and layer thickness supports our use of the BSE-based $^{230}Th/^{232}Th$ ratio to correct for initial ^{230}Th. However, we do not use the layer thickness data to derive paleoclimatic information, nor attempt to demonstrate conclusively the layers are truly annual.

[8] The $\delta^{18}O$ and $\delta^{13}C$ values were determined at the University of Massachusetts Stable Isotope Laboratory in 487 subsamples drilled with a 0.5-mm-diameter bit along the stalagmite growth axis at 1-mm intervals, which corresponds to a mean resolution of one sample every 2.9 years (sampling resolution varied from 3.7 yr/sample at the base to 1.0 yr/sample near the tip as a function of growth rate). Each sample integrated ~1.4 years of calcite deposition, thus precluding any potential seasonal aliasing of the isotopic signal. Stalagmite powders were reacted with three drops of anhydrous phosphoric acid at 70°C in a Finnigan Kiel-III automated carbonate preparation device directly coupled to a Finnigan Delta Plus ratio mass spectrometer and values reported in standard permil (‰) notation with respect to VPDB. Internal precision is 0.1‰ for $\delta^{18}O$ and $\delta^{13}C$. The stable isotope data are available at http://www.ngdc.noaa.gov/paleo/paleo.html.

[9] Ages were assigned to stable isotope subsamples according to a polynomial best fit age model of the U-series ages. A linear interpolation was used to subsample statistically the CHIL-1 $\delta^{18}O$ time series at a constant time step of 1 year in order to perform the wavelet analysis (similar results were produced with a spline function). The first reconstructed component successfully captures the majority of the variance in the time series and was subtracted from the original time series to produce a detrended time series, which was subsequently used for wavelet analysis. The wavelet analysis was performed using a Matlab algorithm for a continuous wavelet transform with significance testing, and using a Morlet wavelet with a wave number of 6 to calculate the wavelet spectra and to extract high-frequency (2 to 8 years) variability from the time series. For additional details on the application of wavelets to climatic data, see *Torrence and Compo* [1998].

3. Results

[10] Within Chilibrillo Cave, we measured wet season relative humidity of ~98%, thus indicating saturated air and slight potential for drip water evaporation, a possible confounding effect on stalagmite $\delta^{18}O$ values. Mean above ground wet and dry season relative humidity at nearby Barro Colorado Island is 93 ± 3% and 83 ± 4%, respectively [*Windsor*, 1990]; higher values year round are likely within the Chilibrillo cave environment. Cave temperature was 27.1°C, corresponding to the mean annual temperature. Drip waters are derived from rain falling on a catchment area of <1 km^2; very slow drips (~1 drip/min) were active at the beginning of the 2001 wet season, and limited or inactive during the 2002 dry season, confirming a transit time of less than 1 year through the thin (<10 m) overlying limestone. Drip water samples were not collected for isotope analysis. However, $\delta^{18}O$ values of the nearby Chilibrillo River vary from −4.7% in the dry season (February 2002) to −5.0‰ VSMOW in the wet season (late May, 2002), in close correspondence to the annual mean weighted $\delta^{18}O$ of Panama City rainfall of −4.7‰ (M. S. Lachniet and W. P. Patterson, Use of correlation and multiple stepwise regression to evaluate the climatic

controls on the stable isotope values of Panamanian surface waters, submitted to *Journal of Hydrology*, 2004, hereinafter referred to as Lachniet and Patterson, submitted manuscript, 2004). We suspect drip water $\delta^{18}O$ values to be quite similar.

[11] Analysis of thin sections shows that the stalagmite consists of dense, low-porosity white and clear calcite; no aragonite crystal fabrics are present. Calcite fabric is dominantly columnar and extends across individual laminae. An absence of layer dissolution features along the sampled axis, such as discontinuous or highly irregular laminae, indicate that undersaturated, chemically aggressive drip waters have not likely affected the stalagmite stratigraphy. However, voids <0.5 cm diameter away from the sampled axis are present, and may indicate nondeposition or impact dissolution. The stalagmite began growth over a sand substrate and the base contains sand layers intercalated with calcite. The areas with detrital sand and voids were avoided in the sampling for stable and radiogenic isotopes.

[12] Previous studies have demonstrated the ENSO/climate link in Panama [*Estoque et al.*, 1985; *Enfield and Alfaro*, 1999; Donoso, Panama Canal case study, 2003]. To test further the modern climate/ENSO relationship, we statistically analyzed rainfall records for Alajuela, 3 km north of our study site, for variance in the ENSO band using raw annual, raw monthly, monthly anomaly (measurement minus the monthly mean), 3-month smooth anomaly, 1-year smooth anomaly, and 2.9-year smooth anomaly data sets (the last to match the average sampling resolution of our sample CHIL-1). We note statistically significant variance (at the 95% confidence level) at periods of 2 to 8 years in Alajuela rainfall, which varied somewhat in time and period depending on the input data set. Variance at periods larger than 8 years is not noted, possibly as a result of the short rainfall time series (99 years). ENSO band variance is most apparent between 1900 and 1920, 1930 and 1940, 1955 and 1965, and 1970 and 1990. The prominent decrease in ENSO band variance between 1940 and 1960 noted by *Torrence and Compo* [1998] is also evident in Alajuela rainfall between 1940 and 1955. Although a detailed treatment of the modern ENSO affect in Panama is beyond the scope of this paper, which focuses on a paleoclimatic time series from Panama, these data and previous studies [*Hastenrath*, 1978, 1984; *Ropelewski and Halpert*, 1987; *Linsley et al.*, 1994; *Waylen et al.*, 1996; *Enfield and Alfaro*, 1999; *Giannini et al.*, 2000; Donoso, Panama Canal case study, 2003] support our interpretations for an ENSO-climate link for the prehistorical period covered by our stalagmite $\delta^{18}O$ record.

[13] To evaluate the amount effect in southern Central America, we analyzed rainfall $\delta^{18}O$ as a function of rainfall amount. Precipitation from stations in Costa Rica (~3 years of record) and Panama (14 years excluding outliers and incomplete data, discontinuous over 1968–1996) [*Lachniet and Patterson*, 2002; International Atomic Energy Agency (IAEA), Global Network of Isotopes in Precipitation and Isotope Hydrology Information System, The GNIP database, Release 3, available at http://isohis.iaea.org/, 1998, hereinafter referred to as IAEA, 1998] demonstrate lower (higher) monthly mean $\delta^{18}O$ values during the wet (dry) season ($R^2 = 0.82$, see Figure 3); the seasonal march of $\delta^{18}O$ in rainfall is the inverse of seasonal rainfall amount. The annual weighted mean in Panama is −4.7‰, and seasonal variability is ~8.0‰ (Lachniet and Patterson, submitted manuscript, 2004). Annual weighted $\delta^{18}O$ from Panama show a weaker correlation with rainfall amount ($R^2 = 0.35$), and the correlation with mean surface temperature is weak ($R^2 = 0.06$). Because El Niño events are associated with less wet season rainfall and a weaker CAM, rainfall $\delta^{18}O$ should be higher, such as noted for drought in Bolivia associated with the 1983 El Niño event [*Gonfiantini et al.*, 2001]. However, the discontinuous 14-year time series for Panama does not include $\delta^{18}O$ values for 3 of 4 years of the two most prominent ENSO events of 1982/1983 and 1997/1998, so it is difficult to evaluate the $\delta^{18}O$/El Niño relationship with the sparse analytical data. However, a modeling study [*Vuille et al.*, 2003] demonstrated that reductions in rainfall associated with El Niño events should be reflected by higher $\delta^{18}O$ values in southern Central America. The response of rainfall amount, $\delta^{18}O$, and ENSO in the modern climate record of Central America remains to be fully characterized, but theory and empirical data [*Rozanski et al.*, 1993; *Gonfiantini et al.*, 2001; *Vuille et al.*, 2003, IAEA, 1998] suggest dominance of the amount effect on rainfall $\delta^{18}O$ values.

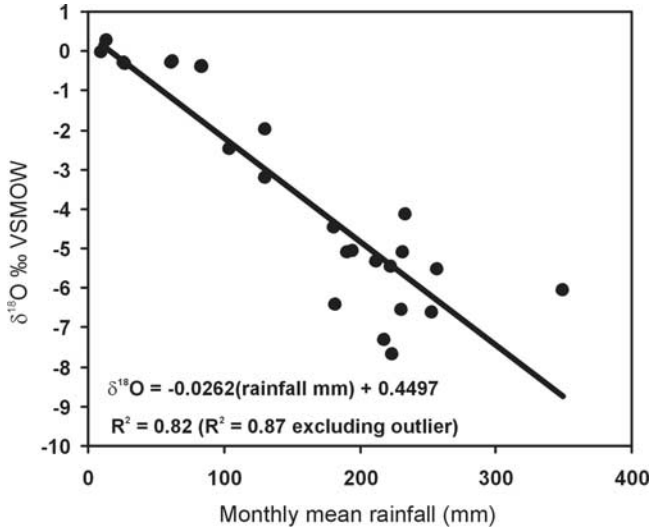

Figure 3. The amount effect in $\delta^{18}O$ values of rainfall in southern Central America. Low (high) $\delta^{18}O$ values are associated with higher (lower) monthly mean rainfall. More intense convection promotes increased rain out of vapor from the cloud and relatively depleted $\delta^{18}O$ values. The R^2 value increases from 0.82 to 0.87 if the data point at 350 mm is excluded.

[14] On the basis of our U/Th chronology, the stalagmite began growth prior to 64 ± 77 years B.C. and continued to ~1310 A.D. (Table 1). Polished sections reveal a hiatus above the youngest U/Th sample that is covered by 12 mm of calcite that accreted to the present beneath the active drip observed in 2002 A.D. The origin of the hiatus is likely from removal of the stalagmite tip by vandalism, because the hiatus displays a jagged and irregular form that cross-cuts the stratigraphy, and no evidence for dissolution of growth layers was noted. On the basis of a sensitivity analysis of our U-series data fitted with several age models,

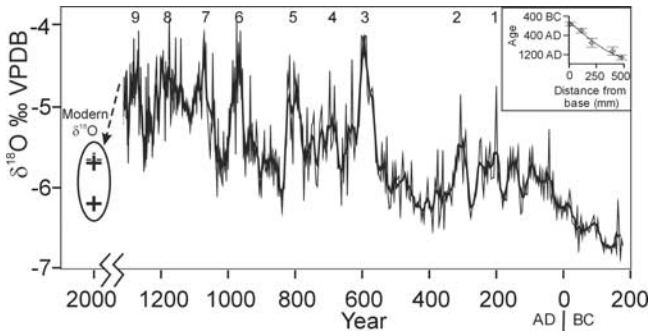

Figure 4. CHIL-1 $\delta^{18}O$ time series. Raw data (thin line) with 5-point (~15 years) running average (thick line). Numbers 1–9 denote dry episodes inferred from peaks in the $\delta^{18}O$ time series. Inset is U/Th age depth relationship and best-fit polynomial age model. Increases in $\delta^{18}O$ values represent drier conditions. Modern calcite $\delta^{18}O$ values represent a return to relatively wetter conditions.

we estimate the timing of isotopic events in our record to be accurate within 50 to 75 year.

[15] The $\delta^{18}O$ values of stalagmite CHIL-1 show large isotopic shifts (Figure 4) that record past variations in rainfall intensity. The $\delta^{18}O$ time series exhibits a millennial-scale trend to higher values, upon which are several pronounced and rapid isotope variations. Two first-order intervals can be recognized in the $\delta^{18}O$ stratigraphy: a less variable interval with lower $\delta^{18}O$ values between 180 B.C. and 550 A.D., and a more variable interval with higher $\delta^{18}O$ values from 550 to 1310 A.D. From 180 years B.C. to 80 A.D., $\delta^{18}O$ values rise monotonically from −6.8 to −5.8‰ with little variability (Figure 4). After 80 A.D. the $\delta^{18}O$ values show 0.5 to 1.0‰ variability until 550 A.D., after which $\delta^{18}O$ values alternate between high and low values with ~1.5 to 2.0‰ variability. Three modern calcite $\delta^{18}O$ values on calcite beneath the drip active in 2002 A.D. range from −5.7 to −6.2‰, and are lower than the 550–1300 A.D. mean of −5.1‰. Nine episodes of high $\delta^{18}O$ values correspond to pronounced rainfall reductions. Episodes one and two occur within the relatively wetter interval at ~200 and 320 A.D., were relatively short-lived, and of smaller magnitude than those that follow. Dry episodes three through nine occur between ~550 and 1300 A.D., respectively, with a centennial-scale pulsing. Higher $\delta^{18}O$ values represent decreased monsoon rainfall intensity within the ITCZ over the site related to either a general weakening of the monsoon or a latitudinal migration of the ITCZ away from the site.

[16] To determine the frequency and temporal variability of isotopic and climatic anomalies, we performed wavelet analysis on the detrended CHIL-1 $\delta^{18}O$ time series (Figure 5). The wavelet spectrum displays variance within the 2- to 8-year ENSO, decadal, and centennial bands, which exceed the 95% confidence level for a red noise

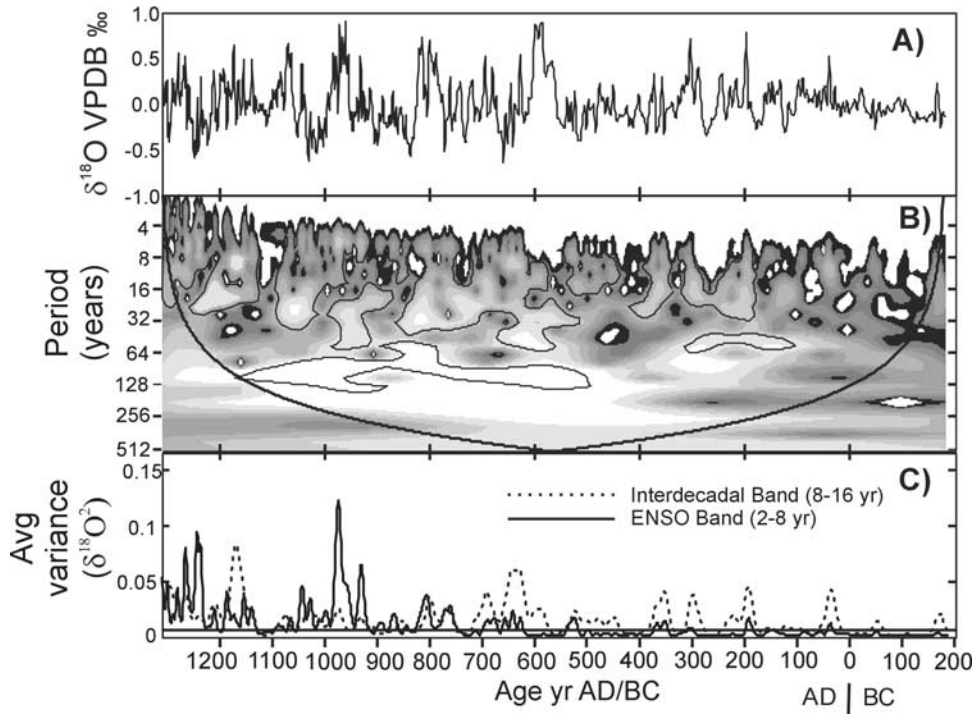

Figure 5. Wavelet spectral analysis of CHIL-1 $\delta^{18}O$ values. (a) Detrended time series. (b) $\delta^{18}O$ wavelet power spectrum. Black to white shades indicate increasing variance; the black contour denotes variance that exceeds the 95% confidence level for a red noise process. Significant variance is evident in the ENSO (2–8 years), interdecadal (8–16 years), and centennial (~80 to 200 years) bands. (c) Scale-averaged wavelet power derived from the ENSO band (solid line) and interdecadal band (dashed line). The horizontal line at the base of the plot is the 95% confidence level. ENSO band variance is highest after ~550 A.D. and corresponds to drier conditions.

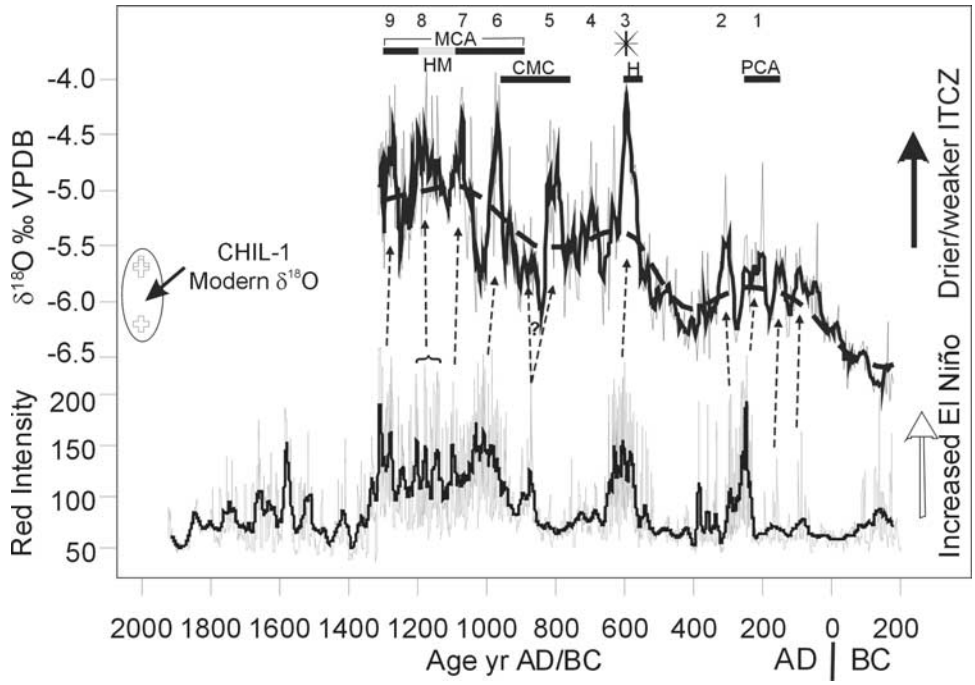

Figure 6. CHIL-1 and Laguna Pallcacocha time series. Top shaded line is raw CHIL-1 $\delta^{18}O$; top solid line is 5-point running average. The dashed black line is the first reconstructed EOF determined from single spectrum analysis. Bottom shaded line is red color intensity, and bottom solid line is the running average of Laguna Pallcacocha core, shifted 75 years older within the error of the age model. The star indicates eruption of Barú Volcano, Panama. Increases in $\delta^{18}O$ coincide with pulses of El Niño activity in Ecuador, evidence that periods of El Niño correspond to a weaker monsoon in Panama. Arrows are correlations; MCA is Medieval Climatic Anomaly; HM is High Medieval; CMC is Classic Maya Collapse; H is Maya Hiatus; and PCA is pre-Classic abandonment.

process with a lag-1 coefficient of 0.85. Sampling resolution generally decreases with age, so ENSO band variance is most prominent at the end of our record. Similar results were obtained with different age models. The wetter and more stable interval from 180 B.C. to 550 A.D. is characterized by small isotopic variance. After 550 A.D. the ENSO band variance increases, coinciding with the drier and more variable interval inferred from the raw $\delta^{18}O$ time series. Significant variance is also present in the multi-decadal to centennial timescales, particularly after 500 A.D, when abrupt drying events of approximately 50- to 100-year duration were separated by wet events of approximately 100- to 150-year duration. The interdecadal band (8–16 years) variance is present throughout the time series, and exhibits a centennial-scale pulsing.

[17] To evaluate further the extent to which ENSO is related to rainfall variability over Panama, we compared the CHIL-1 $\delta^{18}O$ time series with an El Niño proxy record from Laguna Pallcacocha, Ecuador [*Moy et al.*, 2002]. In the Laguna Pallcacocha watershed, slope erosion is triggered by heavy rainfall associated with moderate to strong El Niño events, and resulting clastic layers are preserved in the lake sediments [*Rodbell et al.*, 1999]. There is a strong correspondence between El Niño variability recorded in Laguna Pallcacocha and high $\delta^{18}O$ value (dry) episodes in sample CHIL-1 (Figure 6), such that individual pulses in El Niño activity have counterparts in weak monsoon periods in Panama. On the basis of this correspondence and statistically significant variance in the ENSO band described above, we infer that ENSO has been active in southern Central America over the interval of our record.

4. Discussion

[18] We observe that $\delta^{18}O$ values in CHIL-1 show a broad increase (drying) from 180 B.C. to 1310 A.D., a trend that is not apparent in the Pallcacocha record (which may be an on/off type of recorder of ENSO). The broad drying trend in CHIL-1 may be related to insolation-forced drying of the tropics [*Haug et al.*, 2003] or some other control on monsoon rainfall. $\delta^{18}O$ data of planktic foraminifera from the Cariaco Basin are interpreted to reflect a gradual cooling of late summer-fall SSTs in the southern Caribbean Sea [*Black et al.*, 2004]. Such a long-term cooling of Caribbean SSTs could have resulted in a shorter wet season in Panama [*Enfield and Alfaro*, 1999], and may explain the long-term trend to drier conditions inferred from the CHIL-1 $\delta^{18}O$ time series. Further, periods of increased El Niño event frequency in Ecuador coincide with stepwise increases in mean $\delta^{18}O$ in CHIL-1 (Figure 6). Lower modern CHIL-1 $\delta^{18}O$ values ($\sim -6.0‰$) are consistent with a return to relatively wetter conditions in Panama related to decreasing El Niño activity. Increased variance within ENSO bandwidths after 550 A.D. is associated with more variable rainfall, and likely reflects increased ENSO activity in the eastern Pacific Ocean. We do not find a 208-year drought cycle, linked to the 206-year solar cycle, as determined by *Hodell et al.* [2001] from bulk density measurements in sediment from Lake Chichancanab,

Mexico, and noted at other sites in the Caribbean region [*Nyberg et al.*, 2001]. Nor do we observe a correspondence between our record and solar-forced variations in atmospheric $\Delta^{14}C$ values from tree rings and other proxy records [*Stuiver et al.*, 1998]. Taken together, our data suggest that ENSO, and not solar variability, is the primary driver of hydrologic anomalies in the Panama Canal Zone, and by extension perhaps much of the Pacific Coast of Central America. We suggest that interdecadal- to centennial-scale variations in eastern Pacific SSTs and ENSO may obscure any signal of the 11-year and 206-year solar cycles that are evident in other Caribbean basin paleoclimate records [*Hodell et al.*, 2001; *Nyberg et al.*, 2001; *Black et al.*, 2004]. However, further records from the region are required to test this possibility.

[19] The $\delta^{18}O$ values of the "modern" calcite are 0.3 to 1.2‰ higher than those expected for equilibrium calcite at a cave temperature of 27°C and a drip water $\delta^{18}O$ value of −4.7% VSMOW from the Panama City rainfall isotope data (Lachniet and Patterson, submitted manuscript, 2004). Possible explanations of the high modern $\delta^{18}O$ values include (1) higher mean annual rainfall $\delta^{18}O$ at Chilibrillo Cave relative to Panama City, (2) that the stalagmite does not accrete carbonate during the wettest, most isotopically depleted season because of drip waters undersaturated in calcite, or (3) kinetic effects from evaporation and/or rapid CO_2 degassing. Results from $\delta^{18}O$ values in surface waters across the isthmus indicate generally decreasing $\delta^{18}O$ values from the Caribbean to the Pacific coasts (Lachniet and Patterson, submitted manuscript, 2004), so Chilibrillo may have a higher mean annual rainfall $\delta^{18}O$ value. Surface water $\delta^{18}O$ values near Chilibrillo Cave (n = 4; −4.7 to −5.0‰ VSMOW), however, are quite near the Panama City mean $\delta^{18}O$ value (−4.7‰ VSMOW) so we cannot evaluate fully this possibility. Although evaporation of drip water in the cave should be minimal given the high drip-season relative humidity, evaporation of water in the soil zone is possible. Such evaporation would increase the $\delta^{18}O$ value of drip water before reaching the stalagmite. Land clearance above the cave could conceivably increase soil water evaporation by removal of arboreal vegetation, but we cannot independently assess this possible effect on our isotope stratigraphy. The absence of layer dissolution features in thin section indicates that undersaturated, chemically aggressive drip waters have not likely affected the sampled isotope stratigraphy. Further, columnar calcite crystals extend across regular dark/light laminae couplets, indicating no significant interruption of calcite accretion, and we infer that our sample deposited calcite throughout the drip season. Rapid CO_2 degassing would result in increased $\delta^{18}O$ and $\delta^{13}C$ values, and may explain the discrepancy. The $\delta^{13}C$ values from CHIL-1 increase from −10‰ at 200 B.C. to near 0‰ at ∼1300 A.D., upon which is superimposed 2 to 3‰ subdecadal- to centennial-scale variability. The large $\delta^{13}C$ trend to higher values may indicate a decreased proportion of isotopically light respired CO_2 to the drip water as a result of agricultural land clearance above the cave, whereas the higher-frequency variability may be related to variation in soil respiration rates [*Frappier et al.*, 2002].

[20] Stalagmite $\delta^{13}C$ values may also record rainfall variations above the cave; increased rainfall would promote biologic respiration and a greater proportion of isotopically depleted biogenic CO_2 to drip waters [*Burns et al.*, 2002]. Conversely, relatively drier periods may result in a thinner water film on the stalagmite tip because of slower drip water delivery, from which CO_2 degassing may proceed more rapidly. The CHIL-1 anomaly $\delta^{18}O$ and $\delta^{13}C$ values are moderately correlated (R^2 = 0.53), suggesting a common forcing mechanism for some of the covariation. We suggest that rainfall-related variations in biogenic respiration and/or kinetic effects from CO_2 degassing are responsible. Both possible effects act in the same direction as the amount effect and would amplify the climatic signal [*Burns et al.*, 2002]. In consideration of these effects, we restrict our interpretations to qualitative statements of wet/dry.

[21] The CHIL-1 $\delta^{18}O$ data also provide paleoclimate information relevant to cultural changes in Central America and elsewhere. For example, dry episodes one and two happen near the time of the Maya pre-Classic abandonment (Figure 6). Episode three at 560–630 A.D. coincides with the Maya Hiatus, increased El Niño activity in Ecuador, and a massive eruption of the Barú Volcano in western Panama, after which time pre-Colombian habitation of the volcano flanks ceased until 1200 A.D. [*Linares et al.*, 1975]. While previously attributed to this volcanic catastrophe, we find that cultural abandonment of Barú Volcano's slopes happened concurrently with a monsoon weakening. Two pronounced dry episodes in Panama between ∼770 and 1010 A.D. (dry episodes five and six) coincide with the Classic Maya Collapse [*Webster*, 2002] from 750–950 A.D. Our data provide evidence that southern Central America also experienced drier conditions coincident with cultural changes in northern Central America, but a direct climatic teleconnection between the areas is inferential. Further, the dry periods are associated with more variable rainfall and increased ENSO band variance in Panama (Figure 5). Initial drying in Panama began 200 years before and extended at least 350 years after the Classic Maya Collapse evident in northern Central America [*Curtis et al.*, 1996; *Hodell et al.*, 2001], and was punctuated by several returns to relatively less dry conditions. In contrast to the Maya, cultures in Costa Rica and Panama experienced an efflorescence after 800 A.D. [*Cooke*, 1984], suggesting a different cultural response to more variable rainfall.

[22] Our data also show pronounced hydrologic anomalies during Medieval time, particularly during the 1100–1200 A.D. "High Medieval" [*Bradley et al.*, 2003] when western European temperatures were anomalously high. Rainfall anomalies began as early as 550 A.D. in Panama (Figure 6), but the driest conditions occurred between 900 and 1310 A.D. The correspondence between warm medieval temperatures and dry hydrologic anomalies in Panama supports a large-scale Medieval Climatic Anomaly that may have been global in extent, and involved atmospheric circulation reorganizations that are linked to ENSO.

[23] The presence of prehistorical dry periods in Panama also has important implications for contemporary time. For example, the lower $\delta^{18}O$ values of modern calcite on CHIL-1 suggest that the recent climate in Panama is wetter than the 550–1300 A.D. period. If the past is an indication of future climate changes, the occurrence of El Niño droughts apparent in the CHIL-1 $\delta^{18}O$ record suggest that future dry periods in Panama are also possible. Because the

Panama Canal and most residents of Central America rely upon on monsoon rainfall to fill the lock system, generate hydroelectric power, and provide drinking water, future dry events may have unfavorable effects on canal operation and public water supplies.

[24] **Acknowledgments.** Fieldwork was supported by a postdoctoral fellowship from the Smithsonian Tropical Research Institute in Panama to M.S.L. and analyses by NSF grants ATM-0318172 to M.S.L. and S.J.B. and ATM-0317654 to Y.A. We thank José Iriardo from STRI for assistance in fieldwork and Keely Brooks and David Weide for reviews of earlier drafts of this manuscript. We also thank three reviewers for helpful comments that improved the manuscript.

References

Black, D. E., R. C. Thunell, A. Kaplan, L. C. Peterson, and E. J. Tappa (2004), A 2000-year record of Caribbean and tropical North Atlantic hydrographic variability, *Paleoceanography*, *19*, PA2022, doi:10.1029/2003PA000982.

Bradley, R. S., M. K. Hughes, and H. F. Diaz (2003), Climate in medieval time, *Science*, *302*, 404–405.

Burns, S. J., D. Fleitmann, M. Mudelsee, U. Neff, A. Matter, and A. Mangini (2002), A 780–year annually resolved record of Indian Ocean monsoon precipitation from a speleothem from south Oman, *J. Geophys. Res.*, *107*(D20), 4434, doi:10.1029/2001JD001281.

Cobb, K. M., C. D. Charles, H. Cheng, and R. L. Edwards (2003), El Niño/Southern Oscillation and tropical Pacific climate during the last millennium, *Nature*, *424*, 271–276.

Cooke, R. (1984), Archeological research in central and eastern Panama: A review of some problems, in *The Archaeology of Lower Central America*, edited by F. W. Lange and D. Z. Stone, pp. 263–302, Univ. of N. M. Press, Albuquerque.

Curtis, J. H., D. A. Hodell, and M. Brenner (1996), Climate variability on the Yucatan Peninsula (Mexico) during the past 3500 years, and implications for Maya cultural evolution, *Quat. Res.*, *46*, 37–47.

Enfield, D. B., and E. J. Alfaro (1999), The dependence of Caribbean rainfall on the interaction of the tropical Atlantic and Pacific oceans, *J. Clim.*, *12*, 2093–2103.

Estoque, M. A., J. Luque, M. Y. Chandeck-Monteza, and J. García (1985), Effects of El Niño on Panama rainfall, *Geofis. Int.*, *24*, 355–381.

Fleitmann, D., S. J. Burns, M. Mudelsee, U. Neff, J. Kramers, A. Mangini, and A. Matter (2003), Holocene forcing of the Indian monsoon recorded in a stalagmite from southern Oman, *Science*, *300*, 1737–1739.

Frappier, A., D. Sahagian, L. A. González, and S. J. Carpenter (2002), El Niño events recorded by stalagmite carbon isotopes, *Science*, *298*, 565.

Giannini, A., Y. Kushnir, and M. A. Cane (2000), Interannual variability of Caribbean rainfall, ENSO, and the Atlantic Ocean, *J. Clim.*, *13*, 297–311.

Gonfiantini, R., M.-A. Roche, J.-C. Olivry, J.-C. Fontes, and G. M. Zuppi (2001), The altitude effect on the isotopic composition of tropical rains, *Chem. Geol.*, *181*, 147–167.

Hastenrath, S. (1978), On modes of tropical circulation and climate anomalies, *J. Atmos. Sci.*, *35*, 2222–2231.

Hastenrath, S. (1984), Interannual variability and annual cycle: Mechanisms of circulation and climate in the tropical Atlantic sector, *Mon. Weather Rev.*, *112*, 1097–1107.

Haug, G. H., K. A. Hughen, D. M. Sigman, L. C. Peterson, and U. Röhl (2003), Southward migration of the Intertropical Convergence Zone through the Holocene, *Science*, *293*, 1304–1308.

Hendy, C. H. (1971), The isotopic geochemistry of speleothems-1. The calculation of the effects of different modes of formation on the isotopic composition of speleothems and their applicability as palaeoclimatic indicators, *Geochim. Cosmochim. Acta*, *35*, 801–824.

Hodell, D. A., M. Brenner, J. H. Curtis, and T. Guilderson (2001), Solar forcing of drought frequency in the Maya lowlands, *Science*, *292*, 1367–1370.

Lachniet, M. S., and W. P. Patterson (2002), Stable isotope values of Costa Rican surface waters, *J. Hydrol.*, *260*, 135–150.

Lamb, H. H. (1965), The Early Medieval Warm epoch and its sequel, *Palaeogeogr. Palaeoclimatol. Palaeoecol.*, *1*, 13–37.

Linares, O. F., P. D. Sheets, and E. J. Rosenthal (1975), Prehistoric agriculture in tropical highlands, *Science*, *187*, 137–145.

Linsley, B. K., R. B. Dunbar, G. M. Wellington, and D. A. Mucciarone (1994), A coral-based reconstruction of Intertropical Convergence Zone variability over Central America since 1707, *J. Geophys. Res.*, *99*, 9977–9994.

Moy, C. M., G. O. Seltzer, D. T. Rodbell, and D. M. Anderson (2002), Variability of El Niño/Southern Oscillation activity at millennial timescales during the Holocene epoch, *Nature*, *240*, 162–165.

Nyberg, J., A. Juikpers, B. A. Malmgren, and H. Kunzendorf (2001), Late Holocene changes in precipitation and hydrography recorded in marine sediments from the northeastern Caribbean Sea, *Quat. Res.*, *56*, 87–102.

Polyak, V. J., and Y. Asmerom (2001), Late Holocene climate and cultural changes in the southwestern United States, *Science*, *294*, 148–151.

Richards, D. A., and J. A. Dorale (2003), Uranium-series and environmental applications of speleothems, *Rev. Mineral. Geochem.*, *52*, 407–460.

Rodbell, D. T., G. O. Seltzer, D. M. Anderson, M. B. Abbott, D. B. Enfield, and J. H. Newman (1999), An ~15,000–yr record of El Niño-driven alluviation in southwestern Ecuador, *Science*, *283*, 516–520.

Ropelewski, C. F., and M. S. Halpert (1987), Global and regional scale precipitation patterns associated with the El Niño/Southern Oscillation, *Mon. Weather Rev.*, *115*, 1606–1626.

Rozanski, K., L. Araguás-Araguás, and R. Gonfiantini (1993), Isotopic patterns in modern global precipitation, in *Climate Change in Continental Isotopic Records*, *Geophys. Monogr. Ser.*, vol. 78, edited by P. K. Swart et al., pp. 1–36, AGU, Washington, D. C.

Stine, S. (1994), Extreme and persistent drought in California and Patagonia during mediaeval time, *Nature*, *369*, 546–549.

Stuiver, M., P. J. Reimer, E. Bard, J. W. Beck, G. S. Burr, K. A. Hughen, B. Kromer, F. J. McCormac, J. van der Plicht, and M. Spurk (1998), INTCAL radiocarbon age calibration, 24,000–0 cal. yr BP, *Radiocarbon*, *40*, 1041–1083.

Torrence, C., and G. P. Compo (1998), A practical guide to wavelet analysis, *Bull. Am. Meteorol. Soc.*, *79*, 61–78.

Vuille, M., R. S. Bradley, M. Werner, R. Healy, and F. Keimig (2003), Modeling $\delta^{18}O$ in precipitation over the tropical Americas: 1. Interannual variability and climatic controls, *J. Geophys. Res.*, *108*(D6), 4174, doi:10.1029/2001JD002038.

Waylen, P. R., C. N. Caviedes, and M. E. Quesada (1996), Interannual variability of monthly precipitation in Costa Rica, *J. Clim.*, *9*, 2606–2613.

Webster, D. (2002), *The Fall of the Ancient Maya*, 368 pp., Thames and Hudson, London.

Windsor, D. M. (1990), Climate and moisture availability in a tropical forest: Long-term records from Barro Colorado Island, Panama, *Smithson. Contrib. Earth Sci.*, *29*, 1–144.

Y. Asmerom and V. J. Polyak, Department of Earth and Planetary Sciences, University of New Mexico, Albuquerque, NM 87131, USA.

S. J. Burns, Department of Geosciences, University of Massachusetts, Amherst, MA 01003, USA.

K. Christenson, 2012 Peach Orchard Drive, Apt. 24, Falls Church, VA 22043, USA.

M. S. Lachniet, Department of Geoscience, University of Nevada, 4505 Maryland Parkway, Box 4010, Las Vegas, NV 89154, USA. (matthew.lachniet@ccmail.nevada.edu)

C. M. Moy, Department of Geological and Environmental Sciences, Braun Hall, Bldg. 320, Stanford University, Stanford, CA 94305, USA.

D. R. Piperno, Smithsonian Tropical Research Institute, APO AA 34002-0948, Republic of Panama.